Development of a PPG-based hardware and software system deployable on elbow and thumb for real-time estimation of pulse transit time

Development of a PPG-based hardware and software system deployable on elbow and thumb for real-time estimation of pulse transit time

Andrea Valerio*, Adhurim Hajzeraj, Omid Varnosfaderani Talebi,
Marco Belcastro, Salvatore Tedesco, Danilo Demarchi, Brendan O'Flynn

***Abstract*— Blood pressure (BP) is a vital parameter used by clinicians to diagnose issues in the human cardiovascular system. Cuff-based BP devices are currently the standard method for on-the-spot and ambulatory BP measurements. However, cuff-based devices are not comfortable and are not suitable for long-term BP monitoring. Many studies have reported a significant correlation between pulse transit time (PTT) with blood pressure. However, this relation is impacted by many internal and external factors which might lower the accuracy of the PTT method. In this paper, we present a novel hardware system consisting of two custom photoplethysmography (PPG) sensors designed particularly for the estimation of PTT. In addition, a software interface and algorithms have been implemented to perform a real-time assessment of the PTT and other features of interest from signals gathered between the brachial artery and the thumb. A preclinical study has been conducted to validate the system. Five healthy volunteer subjects were tested and the results were then compared with those gathered using a reference device. The analysis reports a mean difference among subjects equal to -3.75±7.28 ms. Moreover, the standard deviation values obtained for each individual showed comparable results with the reference device, proving to be a valuable tool to investigate the factors impacting the BP-PTT relationship.**

***Clinical Relevance*— The proposed system proved to be a feasible solution to detect blood volume changes providing good quality signals to be used in the study of BP-PTT relationship.**

I. Introduction

Hypertension, or elevated blood pressure (BP), is a medical condition that significantly increases the risks of coronary heart disease such as stroke and heart failure [1]. Several methods for measuring BP are nowadays accessible. Catheterization, auscultation, oscillometry, and volume clamping are the most common techniques used in clinical practice currently [2]. Catheterization is the gold standard procedure. However, this is an invasive method that requires a trained clinician to be performed and can cause severe pain to the patient. Despite their popularity and usability, all non-invasive inflatable cuff-based approaches are cumbersome and obtrusive for long-term BP monitoring. Several studies and research initiatives have been conducted to discover novel cuff-less methods of measuring BP [3]–[6] to better understand and define significant predictors useful to identify asymptomatic organ damage (OD) [7] and evaluate any cardiovascular risk. Arterial stiffness is a strongly associated indicator as regards the status of the cardiovascular system [8]. Particularly, arterial stiffness is associated with the elastic characteristics of the arteries, and it plays a crucial role in systolic BP measurements [9]. Hughes *et al.* [10] defined the relationship between the cardiovascular elasticity, *E*, and BP as

$$E = E_0 e^{\alpha P} \tag{1}$$

Where E_0 is the elastic modulus of the arterial wall of the subject when the pressure is equal to zero, *P* is the mean value of the BP and α is a correction factor. According to the Moens-Korteweg equation [11], pulse wave velocity (PWV), was correlated to the arterial stiffness of the vessel as follows:

$$PWV = \sqrt{\frac{hE}{2r\rho}} \tag{2}$$

Where *h* represents the thickness of the vessel, *r* the radius of the vessel and ρ is the density of the blood. However, PWV is also defined as the velocity required for the pressure wave to propagate between two sites in the cardiovascular system, e.g.

$$PWV = \frac{d}{PTT} \tag{3}$$

Where d is the distance between the two sites and the pulse transit time (PTT) is the time required for the pressure wave to travel from the first to the second site. Combining Eq. (1), (2), (3), and expressing (3) in terms of PTT we obtain the following relationship which links PTT to BP:

$$PTT = \frac{d}{\sqrt{\frac{hE_0 e^{\alpha P}}{2r\rho}}} \tag{4}$$

Equation 4 establishes an inverse relationship between PTT and BP. The local blood flow regulation [14], non-uniform artery diameter between the heart and the peripheral point [15], and reflection phenomena caused by arteries branches [6] are known factors influencing the BP-PTT relationship. To minimize the influence of the factors listed above, in this work PTT is estimated from two PPG sensors, located on the elbow and thumb, instead of an ECG and a PPG sensor [12]. In this way the source of error related to the inclusion of the Pre-Ejection-Period (PEP) [13] was avoided.

This publication has emanated from research supported by a research grant from the Disruptive Technologies Innovation Fund (DTIF) project HOLISTICS funded by Enterprise Ireland (EI). Aspects of this research have emanated from research conducted with the financial support of Science Foundation Ireland under Grant 12/RC/2289-P2-INSIGHT and 16/RC/3918-CONFIRM, which are co-funded under the European Regional Development Fund.

All authors are with the Tyndall National Institute, University College Cork, Lee Maltings Complex, Dyke Parade, T12R5CP Cork, Ireland

Andrea Valerio and Danilo Demarchi are also with the Department of Electronics and Telecommunications, Politecnico di Torino,10129 Torino, Italy (e-mail: andrea.valerio@polito.it; danilo.demarchi@polito.it).

*Corresponding author. e-mail: andrea.valerio@polito.it

The time required for the pulse to propagate between the two sites represents the PTT in this case. The main principle of operation is that by choosing a short, uniform and easily accessible section located as close as possible to the heart, the influence of arterial branches and non-uniform artery size may be reduced in terms of the BP-PTT relationship. The Biosignal acquisition system [18] (Biosignal Plux, Lisboa, Portugal), has been used as reference device to retrieve the raw data from the mentioned acquisition sites and compare the output of the PTT assessment. This system consists of two reflective PPG sensors with two emitting LEDs, one in the red and the other in the infrared (IR) regions of the spectrum. A photodiode placed on each sensor absorbs the reflected light of each one of these LEDs and converts it into a digital output. Through the dedicated software OpenSignals, the sampling frequency of the sensors has been set at 500 Hz. Through the same software, the light intensity of both LEDs was configured on each acquisition site. The structure of this article is as follows. In Section II, the proposed system's hardware, software, and clinical user process are described. Comparing the proposed system to the clinical gold-standard equipment for BP assessment, Section III presents the evaluation results achieved followed by a relevant discussion and conclusion.

II. The Proposed System

This section describes the components of the system developed to evaluate and test the hypothesis described in the previous section, e.g., the custom PPG sensor system designed to capture the signal from larger arteries, the bespoke mechanical fixture designed to control the pressure applied on the skin, and the software for signal processing and data visualisation.

A. The Hardware

In this work, PPG sensors were used to assess variations in blood volume between the brachial artery and the thumb. To retrieve a good quality PPG signal from the brachial artery, brighter LEDs and more sensitive photodiodes have been employed compared to the conventional wrist-based PPG sensors. A PPG sensor includes DAC LED drivers (AFE), ADC Photodiode (PD) signal acquisition, LEDs, Photodiodes (PDs), and an optional ambient light cancellation (ALC). Because of their size, power consumption, and adaptability, integrated PPG sensors are more suited for wearable applications. Among the types of integrated PPG sensors available in the market, an integrated sensor which allows for connection with external LEDs and photodiodes (PDs) has been selected for our purpose. The MAX86141 (Maxim Integrated, San Jose, USA) from Maxim Integrated was chosen as the PPG sensor after analyzing all constraints as size, power consumption, adaptability, and availability. The MAX86141 is an ultra-low power, fully integrated, optical data acquisition system. On the transmitter side, it has three programmable high-current LED drivers, and on the receiver side, it has two optical readout channels that can operate simultaneously. The device includes a low noise signal conditioning analog front-end (AFE) with a 19-bit ADC and an ambient light cancellation (ALC) circuit. The MAX86141 can carry out sampling at frequencies of up to 4096 samples per second. For our application, the sampling rate was set at 500 Hz to allow real-time data processing while ensuring an adequate time resolution (2 ms). Due to limited number of studies on the penetration of light within the body when used for obtaining PPG from the brachial artery, the initial prototype employs LEDs of varying wavelengths to define the optimum wavelength to be used. The SFH 7015 (Osram Licht AG, Munich, Germany) contains a hyper red LED and a 940nm infrared LED along with a Green LED CT DBLP31.12 (Osram Licht AG, Munich, Germany) were also used. Up to two external photodiodes can be connected to MAX86141. According to the selected LEDs, at least one of them should be capable to receive infrared light under a variety of conditions. In this regard, VEMD5080X01 (Vishay Intertechnology Inc., Malvern, USA) from Vishay has been chosen for receiving IR and red light. Vishay's VEMD5510CF and Osram's SFH 2713 contain IR cut filters and can pass light up to 670nm, hence they can only be used with green LEDs. The system employs an ultra-low power consumption microcontroller capable of simultaneously handling real-time sensor reading along with data transfer to the dedicated graphical user interface. STM32WB55CGU6 (STMicroelectronics, Geneva, Switzerland) is a dual-core, multi-protocol, and ultra-low-power 2.4 GHz MCU system-on-chip developed by ST Microelectronics. This device is meant to be exceptionally low-power, with a high-performance Arm® Cortex®-M4 32-bit core working at up to 64 MHz. The entire system is powered by one of the available 5V COM-Port on the laptop used to run the software responsible for the PTT assessment. A USB-C cable is used to power and control the device, allowing reliable data transmission. Two LDO regulators from the NCP170 (ON Semiconductor, Phoenix, USA) family of ON Semiconductor have been employed to provide the correct working supply voltage required by all the components belonging to the system. This LDO family drop-out voltage is 170mV and the quiescent current for the NCP170 series is very low. The reduced dimensions of the selected packaging XDFN4 (1mm x 1mm), make this family ideal for wearable applications. NCP170AMX190TCG generates 1.9V which keeps enough margin from the maximum and the minimum supply voltages of all components. Another regulator is NCP170AMX310TCG which generates 3.1V and the main reason for having this is to provide the supply voltage for LEDs and LED drivers of PPG sensors.

B. Mechanical Design to Control the Contact Pressure

During the creation of the proposed device, Figure 1 (a), the design of the enclosure housing the hardware described in the preceding section was given careful consideration. The design was created to guarantee that the sensor adheres to the sample site, applying steady pressure and avoiding the presence of the operator to keep it in its position. This feature enables the user to reproduce the acquisition

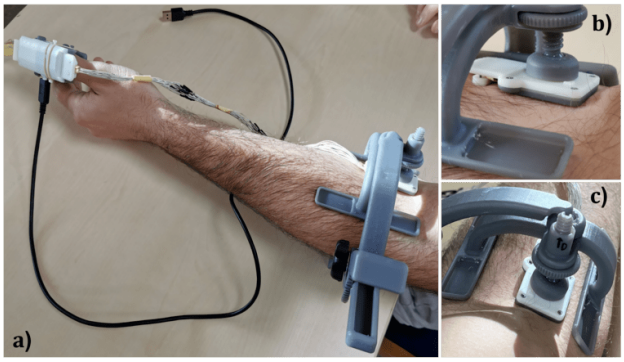

Fig. 1. (a) Blood pressure device applied on the subject. (b) Rotating wheel used to ensure the contact between the PPG sensor and the brachial artery. (c) Elbow's sensor placed on the brachial artery.

Fig. 2. 3D printed enclosures realized for the blood pressure device. Support containing the elbow's sensor (left). Finger clip holding the thumb sensor (right).

Fig. 3. Graphic User Interface used by the device in the blood pressure assessment. The upper plots show the thumb signal (red) and elbow signal (blue). Bottom plots depict the intersecting tangent being extracted from gathered signals for PTT estimation.

setup for a particular subject, hence improving measurement reproducibility. Figure 2 depicts both the fabricated supports and their placement on the subject's body during data collection. The thumb-mounted holder, Figure 2 (right), resembles the design of a standard pulse oximeter. The presence of an elastic spring allows the sensor to adhere to the finger. Figure 2 (left) shows the sensor holder positioned on the elbow. The side structure allows the operator to adjust the pressure exerted on the arm, Figure 1 (c). Through a graduated scale, it is possible to note the opening set for each subject. The sensor has been placed in the upper section of the holder. As shown in Figure 1 (b), the location of the latter can be modified vertically using a rotating wheel while the sensor's orientation relative to the vessel can be adjusted using a spherical head that permits sensor rotation. All the enclosures presented have been designed using the SolidWorks environment (Dassault Systèmes SE, Vélizy-Villacoublay France) and 3D printed using a Formlab 3 printer (Formlabs, Somerville, USA).

C. Algorithm

The datasets gathered by the system, stored in synchronized buffers, are sent through a USB cable connection to the laptop running the algorithm used for the real-time processing. Using one of the COM ports available on the workstation, the graphic user interface (GUI) can receive, visualise and manage the data transferred by the device. Real-time acquisition, display of samples and PTT computation are made possible thanks to a multi-thread process involving two buffers, named respectively acquisition buffer and processing buffer.

The GUI is divided into four different plots and a separate box showing the real-time update of the computed features Figure 3. The first two plots are used to display the acquired signals while the last two depict the result of the application of the algorithm used to compute the PTT on each pulse. This feature is later used to compute the systolic blood pressure (SBP), the diastolic blood pressure (DBP), and heart rate (HR) in a 6 seconds window. The user interface allows the user to store the collected raw data and extracted features in a separate file for later study. The aim of the algorithm employed by the developed system is the extraction of a characteristic that detects the passage of the pulse throughout each cardiac cycle. Specifically, among the several foot-to-foot algorithms reported in the literature, the intersecting tangent method has been chosen for our purpose since it has been shown to be the most reliable method for PTT estimation [16]. This technique consists of the detection of the intersection between the horizontal line passing through the minimum that precedes the systolic peak and the tangent line to the ascending part of the signal. The application of several filter steps to remove the DC-bias and the high-frequency noise affecting the signal. To accomplish this, a 4th-order Chebyshev II band-pass filter with cut-off frequencies ranging from 0.5 to 10 Hz was used to process the data. The phase distortion introduced by the usage of the filter was removed by applying the filter twice through forward-backward filtering. The steps constituting the algorithm used to extract the PTT, Figure 4, from the collected signals are reported in detail below.

i) Firstly, the collected signal is separated into epochs of similar length, with a duration of 6 seconds (e.g., 3000 samples @500Hz). According to the subject's heart rate, we expect a range of 4-10 pulses at a frequency between 40 and 100 bpm.

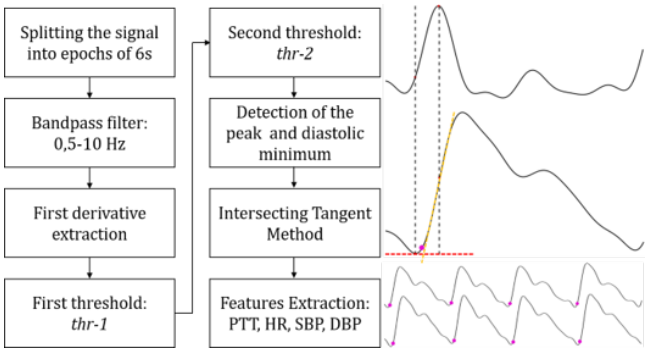

Fig. 4. Flowchart of the algorithm used to compute the PTT.

ii) The signal is filtered with a Chebyshev II band-pass filter of the 4th order with cut-off frequencies of 0.5 and 10 Hz to remove DC offset and high-frequency noise from the signal

iii) Following the pre-processing steps, the analysis of the current window's pulses begins. Firstly, the first derivative of the signal is calculated and then, using two dynamic thresholds, the peaks associated with each pulse are recognized.

iv) The first threshold *(trh-1)* is computed by averaging the positive points within the first derivative of the signal across the entire window.

v) Later, the second threshold *(trh-2)* is determined by averaging the points detected above *trh-1* in the preceding stage. A peak is localized inside the window when a minimum number of samples above *thr-2* are observed. The sample with the largest amplitude is chosen as the local maximum of the first derivative for each pulse. It is then employed to construct the tangent line to each pulse used in defining the intersecting tangent point.

vi) For every pulse, the end of the diastolic phase was determined on the original signal by detecting the zero-derivative point before the maximum on the first derivative. The horizontal line passing through the minimum preceding the ascending part of the systolic phase is used to compute the intersection of the two lines.

vii) Finally, the intersection of the two tangents marks the arrival of the pulse.

viii) The preceding stages are applied to signals collected from both the elbow and the thumb. Every crossing tangent point calculated is paired with its counterpart in the opposite window, and the PTT is computed as the delay between these two locations. The average of each window's retrieved PTT data is then used to calculate the blood pressure readings according to the relationship reported in [17].

III. System Assessment

For the evaluation of the developed device, a study has been undertaken at the Tyndall National Institute in University College Cork (UCC), Ireland. In this experiment, which was approved by the UCC Clinical Research Ethics Committee of the Cork Teaching Hospitals, a comparison

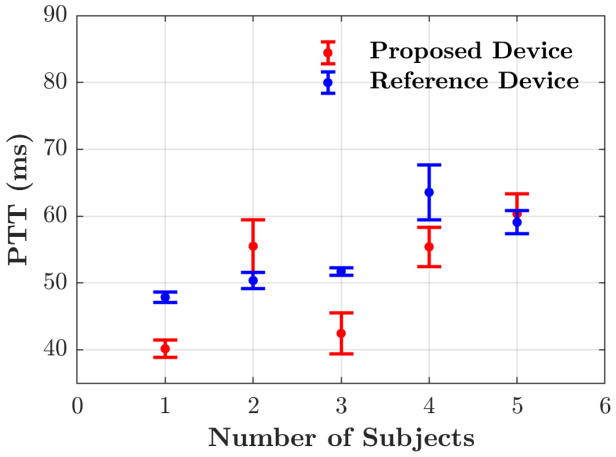

Fig. 5. Averaged PTT values retrieved for the 5 subjects involved in the trial. Each point represents the mean value of the three acquisitions executed with both systems. The error bars report the standard deviation.

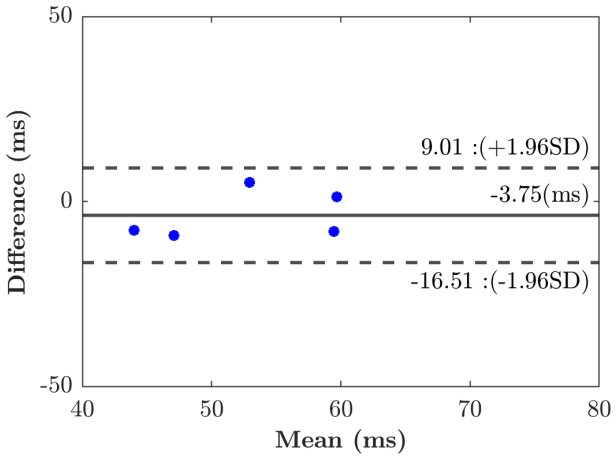

Fig. 6. Bland-Altman plot of the differences between the outcomes retrieved by the reference device and the proposed device.

between the performance of the developed device with that of the Biosignal Plux acquisition system was carried out. As described, the developed device allows for the extraction of the raw data gathered by two PPG sensors applied on the previously mentioned sites, namely, the thumb and elbow. This trial included five volunteer individuals ranging from 23 to 30 years. Table I details the physiological parameters of the people involved. Each data collection was performed in a climate-controlled environment with a temperature set to 20°C. Every individual was asked to refrain from smoking or consuming coffee 30 minutes before the session. After collecting the participant information, the subject was requested to stay supine for 10 minutes to have hemodynamic conditions and vasomotor tone close to baseline level. The next step in gathering PTT data was to locate the two measurement sites such that they do not vary from the reference system to the proposed device. Finally, PTT measurements for each subject at rest were carried out for three consecutive one-minute data captures. Each acquisition was carried out when the patient was seated, with both feet

TABLE I

OVERVIEW OF THE CHARACTERISTICS OF THE STUDY POPULATION

Characteristics	Mean ± s.d.	Range
Number of subjects	5	-
Number of acquisitions	3	-
Male	2 (40%)	-
Age (years)	28 ± 3.27	23-32
Height (cm)	172.2 ± 6.8	164-180
Weight (kg)	66.6 ± 12.3	55-82
BMI (kg m^{-2})	23.56 ± 3.72	17.8-37.11
SBP (mmHg)	108.7 ± 12.03	92-125
DBP (mmHg)	67.2 ± 8.24	56-84
HR (bpm)	-	52-74

Abbreviations: BMI, body mass index, SBP, systolic blood pressure, DBP, diastolic blood pressure, HR, heart rate, bpm, beats per minute, s.d, standard deviation

on the floor and hands on the table at the same level as the heart of the subject. For the system assessment, PTT values retrieved from the real-time application of the algorithm were used. On the other side, the acquisitions gathered using the reference device were processed offline using the procedure described in the previous section. The final PTT values averaged across the three tests are shown in Figure 5 for all the participants; the error bars indicate the measurement dispersion. In Figure 6, the Bland-Altman plot is reported. The PTT mean difference is about -3.75±7.28ms [-16.51 9.01]. Table II provides a summary of the average PTT values acquired by the two devices for each participant, as well as their respective standard deviations (s.d.). From these results, it is clear that the PTT measurements obtained by the proposed device are significantly equivalent to those obtained by the reference system. Moreover, assessing the standard deviation reveals that both systems involved have comparable repeatability.

IV. CONCLUSIONS

In this work, a novel system to perform the real-time estimation of PTT was proposed. The system assessment has been conducted by comparing the measurements obtained by the developed system with those collected from data acquired using a certified off-the-shelf device using PPG sensors. The analysis carried out showed a significant similarity between the outcomes. Furthermore, in two out of five instances, the collected findings on the same individual are of higher reproducibility. However, the study has some limitations. Due to the limited number of available participants, the sample size was smaller than desired. Furthermore, it is important to remember that non-clinical personnel was responsible for the positioning of the sensors. Therefore, it is plausible that a minor displacement of the sensor on the vessel (in the order of mm) could result in a larger disparity between the two devices due to the short distance between the sensors and the speed of the pulse wave in the vessel. The study objective is to demonstrate the viability of using a customized device capable of acquiring and analyzing real-time data with comparable results to the validation device proving to be a valuable tool to investigate the factors impacting PTT and, consequently, its relationship with BP.

TABLE II

SYSTEM ASSESSMENT'S RESULTS

Subjects	PTT (ms)	
	Proposed Device mean ± s.d.	**Reference Device** mean ± s.d.
1	40.1 ± 1.27	47.8 ± 0.78
2	55.5 ± 0.39	50.3 ± 1.18
3	42.4 ± 3.08	51.7 ± 0.52
4	55.4 ± 2.94	63.5 ± 4.13
5	60.3 ± 3	59.1 ± 1.71

Abbreviations: s.d., standard deviation.

REFERENCES

[1] SDGs Sustainable Development Goals. 2022.

[2] A.S. Meidert et al., "Techniques for Non-Invasive Monitoring of Arterial Blood Pressure," Front Med (Lausanne), 4, JAN, 231, 2017.

[3] P. M. Nabeel, et al., "Bi-Modal Arterial Compliance Probe for Calibration-Free Cuffless Blood Pressure Estimation," IEEE Trans Biomed Eng, 65, 11, 2392–2404, 2018.

[4] A. M. Zakrzewski, et al., "Real-Time Blood Pressure Estimation From Force-Measured Ultrasound," IEEE Trans Biomed Eng, 65, 11, 2405–2416, 2018.

[5] A. Chandrasekhar, et al., "Smartphone-based blood pressure monitoring via the oscillometric finger-pressing method," Sci Transl Med, 10, 431, 2018.

[6] R. Mukkamala et al., "Towards Ubiquitous Blood Pressure Monitoring via Pulse Transit Time: Theory and Practice HHS Public Access," IEEE Trans Biomed Eng, 62, 8, 1879–1901, 2015.

[7] B. Williams et al., "2018 ESC/ESH Guidelines for the management of arterial hypertension," Eur Heart J, 39, 33, 3021–3104, 2018.

[8] J. A. Chirinos, et al., "Large-Artery stiffness in health and disease: JACC State-of-the-Art Review," J Am Coll Cardiol, 74, 9, 2019.

[9] J. Wilson et al., "Systolic blood pressure and longitudinal progression of arterial stiffness: A quantitative meta-analysis," J Am Heart Assoc, 9, 17, 17804, 2020.

[10] D. Hughes, "Measurements of Young's modulus of elasticity of the canine aorta with ultrasound," Ultrason Imaging, 1, 4, 356–367, 1979.

[11] N. Westerhof, et al., "The arterial Windkessel," Med Biol Eng Comput, 47, 2, 131–141, 2009.

[12] V. Ganti et al., "Enabling wearable pulse transit time-based blood pressure estimation for medically underserved areas and health equity: Comprehensive evaluation study," JMIR Mhealth Uhealth, 9, 8, 2021.

[13] M. Y. M. Wong, et al., "The effects of pre-ejection period on post-exercise systolic blood pressure estimation using the pulse arrival time technique," Eur J Appl Physiol, 111, 1, 135–144, 2011.

[14] X. Ding, et al., "Continuous Cuffless Blood Pressure Estimation Using Pulse Transit Time and Photoplethysmogram Intensity Ratio," IEEE Trans Biomed Eng, 63, 5, 964-972, 2015.

[15] M. Gao, et al., "Estimation of Pulse Transit Time as a Function of Blood Pressure Using a Nonlinear Arterial Tube-Load Model," IEEE Trans Biomed Eng, 64, 7, 1524, 2017.

[16] I. Buraioli et al., "A New Noninvasive System for Clinical Pulse Wave Velocity Assessment: The Athos Device," IEEE Trans Biomed Circuits Syst, 15, 1, 133, 2021.

[17] V. Figini, et al., "Improving Cuff-Less Continuous Blood Pressure Estimation with Linear Regression Analysis," Electronics (Switzerland), 11, 9, May 2022.

[18] L. M. Rodrigues, et al., "Different lasers reveal different skin microcirculatory flowmotion - data from the wavelet transform analysis of human hindlimb perfusion".